Model-Based Motion Tracking Control of an Electric 3DoF Parallel Motion Platform

M. Aminzadeh
M. Sabzehparvar
Department of Aerospace Engineering
Amirkabir University of Technology
Tehran, Iran
mas.aminzadeh@gmail.com

Abstract—A heave-pitch-roll parallel-type motion platform used extensively for flight simulation applications is considered. [12] It introduces a novel configuration of the mechanism which benefits in two important aspects, better weight balancing due to utilizing a vertically mounted pneumatic actuator and better synchronization and higher stiffness due to the use of a new configuration of scissors. A model-based nonlinear control based on dynamics inversion is applied to the system. Dynamic model of low complexity is employed that describes the predominant dynamics of the system that is appropriate for real-time applications. The controller is then applied to the complete dynamic model that takes into account both the legs' mass and inertia and actuators' frictions. The accuracy of the model is verified by comparison with an equivalent model built in simMechanics. Simulations with typical desired trajectory inputs are presented and a good performance of the controller is achieved with two outstanding properties, an asymptotic convergence of error to zero and a high bandwidth. The bandwidth can further be increased by increasing the break frequency of the derivative filter. In addition, the controlled system presents an overall linear closed loop system that keeps its control specifications in entire the workspace.

TABLE OF CONTENTS

1. INTRODUCTION

Use of a parallel mechanism in flight simulators was first proposed by Stewart in 1965 [1], [2]. It is undoubtedly the most popular motion base for full training simulators. However due to the complexity, difficulty of static weight balancing and control, for early pilot training, prior to the use of full-training simulators, 3dof motion platforms are used which are more cost effective and less energy consuming and the kinematics of the mechanism is further simplified for the purpose of control. In addition, they have been proven to produce motion simulation quality comparable to that produced by a 6DoF Stewart platform [3].

The 3DoF motion platform considered here is a modified heave-pitch-roll platform that can be shown to provide better motion sensation in the pilot compared to its other variants that is implied according to motion cueing algorithms and pilots reports [4],[5]. In addition, this platform can be designed to have parallel structure which benefits from numerous advantages of parallel mechanisms namely higher precision, larger payload capacity and faster motion [6]. Also, in design of the 3DoF platform, a novel balancing system consisting of a vertically mounted pneumatic actuator that is constrained to vertical motion by use of three pairs of scissors has been utilized that provides a better control task due to static weight balancing.

The great nonlinearity inherent with parallel mechanisms has made the control of these systems a matter of concern that has attracted many researchers' attention. The control methods used can be divided into classical control, modern control and intelligent control algorithms. The classical controllers based on PD and PID are simple to implement but keep their performance specifications only in a finite region as a result of linear control being applied to nonlinear dynamics. In recent works many modern and intelligent control techniques such as robust and adaptive controls have been developed for robotic applications. Among the big variety of methods used, model-based computed torque controls are high-performance controllers that have been efficiently used for robotic systems. The computed torque control is used to linearize the system by embedding the inverse dynamics of the system into the controller. The obtained controller also forms the basis for some robust controller design where it is referred to as perfect control [7]-[10].

Although model-based control strategies have been used in robotic applications for long, they have recently been addressed in flight simulation applications and there's still little work in this area. In this article, use of a model-based nonlinear control method is investigated for achieving more accurate motion following that is of vital importance in flight simulation applications [11]. Towards this purpose, a model-based nonlinear controller based on the inverse

[1] 978-1-4244-3888-4/10/$25.00 ©2010 IEEE
[2] IEEEAC paper#1689, Version 1, Updated 2009:12:24

dynamics is applied to the system that compensates for the nonlinearities and dynamics coupling. The proposed controller highly improves the performance in some aspects, namely an asymptotic convergence of error to zero and a considerable increase of bandwidth, depending on the type of numerical derivation of the input. In addition, the controlled system presents an overall linear closed loop system that holds its control specifications in entire the workspace.

In the determination of the controller, the dynamics of the system is modeled and inverted where actuator dynamics and frictions and non uniform distribution of load are taken into consideration. Due to the demand for high-speed motion in the flight simulator, an electrical permanent-magnet (PM) DC servomotor of high power is used that is the most commonly used servomotor in robotic applications [7]. First, the integrated dynamic coupling model is deduced, according to equivalent torques between the mechanical structure and the PM servomotor. Second, model-based inverse dynamics controller is described in detail for the above proposed model. At last a series of numerical simulations are carried out to test the effectiveness of the system and verify the above results.

2. ELECTRICAL MOTION PLATFORM MODELING

Mechanical dynamics

In this section the dynamic model of the 3dof motion platform coupled with its actuation system is developed. Prior to that, a brief description of the mechanism is presented. The 3dof motion platform consists of a platform that is connected to the base by three extensible legs that are actuated by three electrical DC motors. The platform is supported by a vertically mounted pneumatic actuator underneath its center of mass that carries the static load of the platform so that the legs remain unstressed in the neutral condition. Also this special use of the actuator leads to linear damping components in heave direction. The upper universal joint of the pneumatic actuator that is connected to the center of the platform prevents the platform from rotating about the vertical axis and thus constrains the yaw motion. The joint is also constrained to move along a vertical line by utilizing a stiff synchronization mechanism that consists of three pairs of scissors that are synchronized by a gears set at the bottom (see Figure 1). These properties lead to simpler dynamics and better control task compared to analogous 3DoF platforms.

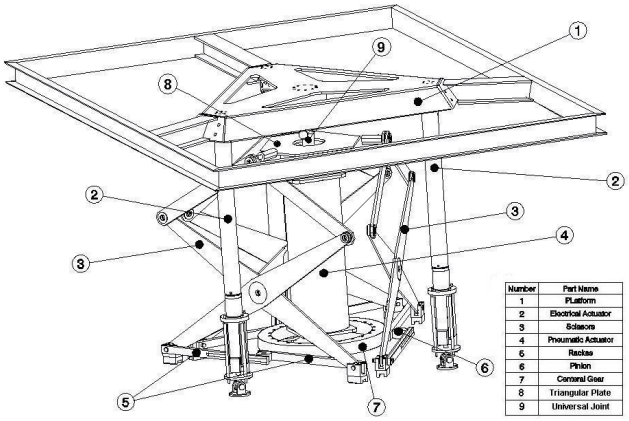

Figure 1-Schematic view of the 3DoF parallel motion platform

By applying the Newton-Euler method to the platform and neglecting the leg's mass and inertia, the dynamics of the system is obtained that like many other robotic systems, can be stated as [7],[12]:

$$M(\bar{x})\ddot{\bar{x}} + V(\bar{x},\dot{\bar{x}}) + G(\bar{x}) + F_{fr}(\dot{\bar{x}}) = \tau, \qquad (1)$$

where $\bar{x} = [z \ \phi \ \theta]^T$ is the 3×1 vector of the platform generalized coordinates, where z is the platform heave coordinate directed downward and φ and θ are the Euler angles. $M(\bar{x})$ is the 3×3 positive definite mass matrix of the system. The 3×1 vector $V(\bar{x},\dot{\bar{x}})$ represents forces/torques arising from centrifugal and Coriolis forces; the 3×1 vector $G(\bar{x})$ represents torques due to gravity, $F_{fr}(\dot{\bar{x}})$ is the 3×1 vector of forces/torques due to friction and τ is the 3×1 vector of applied generalized forces. For detailed information on the derivation of the dynamics of the system see [13]. The defined matrices are summarized in Appendix A.

The above equations are stated in terms of operational variables. If the control is to be done in joint space, the corresponding equations can be obtained by a coordinate transformation [14]. By performing the velocity analysis the following relation is obtained:

$$\dot{\bar{l}} = J\dot{\bar{x}}, \qquad (2)$$

where $\bar{l}$ is the vector of leg lengths (l) and J is the Jacobian matrix. By applying (2) to (1) we obtain:

$$M^*(\bar{x})\ddot{\bar{l}} + V^*(\bar{x},\dot{\bar{x}}) + G^*(\bar{x}) + F_{fr}^*\left(\dot{\bar{l}}\right) = F_a, \qquad (3)$$

where F_a is the 3×1 vector of actuator forces (f_a) and is related to generalized forces through:

$$\tau = J^T F_a. \qquad (4)$$

M^*, V^* and G^* are similar in definition to those defined in

(1) and related to them through the following relations:

$$\begin{aligned} M^* &= (J^T)^{-1} M J^{-1} \\ V^* &= (J^T)^{-1}(V - M\dot{J}\dot{\bar{x}}) \\ G^* &= (J^T)^{-1} G \end{aligned} . \quad (5)$$

$F_{fr}^*\left(\dot{\bar{l}}\right)$ can be assumed to be the summation of viscous and coulomb friction forces as below:

$$F_{fr_j}^*(\dot{l}) = b\dot{l} + f_{k_0}\frac{\dot{l}}{|\dot{l}|}, \quad (6)$$

where b is the viscous friction constant and f_{k_0} is the dry kinetic friction constant for the *j*th actuator.

To solve the dynamic equations (1), solution of kinematics of the system that is embedded in the dynamics, is required. The inverse dynamics of the system is solved through the explicit relations of joint variables vs. operational variables. But solution of the forward kinematics is a little challenging. It requires solution of a set of the nonlinear algebraic equations obtained in inverse kinematics analysis. A common way to address such a problem is Newton-Rophson method which is also used in this paper. But due to the high computational effort caused by many iterative computations involved in this method, another faster approach is taken that is applicable for simulation purposes. Knowing the joint and operational variables at an initial time and the joint variables and their velocities vs. time, operational variables can be obtained from (2) through some explicit algebraic computations and numerical integration which saves much more time for real-time purposes.

B. Actuator dynamics

The servomotor providing the actuation force is a dc permanent-magnet whose dynamics can be described by the following equations [8]:

$$\begin{aligned} v &= R_a i_a + L_a\frac{di_a}{dt} + K_b r\dot{l} \\ J_m r\ddot{l} &= K_a i_a - f_m(\dot{l}) - \frac{f_a}{r} \end{aligned} , \quad (7)$$

where K_a is motor-torque constant, J_m is rotor inertia, R_a and L_a are armature resistance and inductance respectively and K_b is back emf constant. r is gears reduction ratio of the combined motor-ball screw joint with the dimension rad/m, v and i_a are the motor voltage and current. f_m is the torque due to motor friction and is assumed to be equal to viscous friction that can be modeled as $b\dot{l}$ where b is viscous friction constant. The above equations when integrated in the platform dynamics equations yield:

$$\begin{aligned} &\left(M + J^T\left[J_{m_i} r_i^2\right]J^{-1}\right)\ddot{\bar{x}} + \\ &\left(V(\bar{x},\dot{\bar{x}}) + J^T\left[J_{m_i} r_i^2\right]J^{-1}\dot{\bar{x}}\right) + G(\bar{x}) + \left(F_{fr}(\dot{\bar{x}}) + J^T\overline{r_i f_{m_i}}\right) - J^T\left[r_i K_{a_i}\right]\bar{\imath}_a = 0 \\ &\left[L_{a_i}\right]\frac{d\bar{\imath}_a}{dt} = -\left[R_{a_i}\right]\bar{\imath}_a + \left[K_{b_i} r_i\right]\dot{\bar{l}} + \bar{v} \end{aligned} \quad (8)$$

The coupled system is a system with the 3×1 vector of voltages $\bar{v}$ as its input and the 6×1 vector $[\bar{x}^T \quad \bar{\imath}_a{}^T]^T$ as its state where $\bar{\imath}_a$ is the 3×1 vector of currents. The notation $[a_i]$ means $diag\{a_1, a_2, a_3\}$ and $\overline{r_i f_{m_i}} = [r_1 f_{m_1} \quad r_2 f_{m_2} \quad r_3 f_{m_3}]^T$.

3. CONTROLLER DESIGN

In this section a model-based controller is designed for the system. To do so, the system dynamics is inverted i.e. the required force for the system to achieve a desired acceleration in the current state is calculated and the controller output is set equal to that plus a PD combination of error to assure asymptotic convergence of error to zero in the desired manner. Several control schemes for model-based controllers have been proposed [9].

For the electric motion platform, the model-based controller is designed considering the following facts. The trajectory is specified in operational space; therefore the command is in terms of operational variables. The measured variables are in joint space due to the simplicity and low cost of sensors measuring length and length rate i.e. encoders or tachometers compared to accelerometers and gyros required to measure operational variables. Since the measured variables are in joint space, kinematic analyses that depend on geometry must be performed even if the control is done in operational space. Despite this, it can be shown that when control is performed in operational space, kinematic transformation between joint and operational variables that are greatly affected by the system geometry are reduced (see Figure 2); in addition, these transformations appear in such a manner that can be seen to lead to less control error compared to the case when controlled variables are in joint space and operational variables follow the desired command in an open-loop fashion. Following the above conclusions, the best control scheme to use is equivalent to Figure 2a.

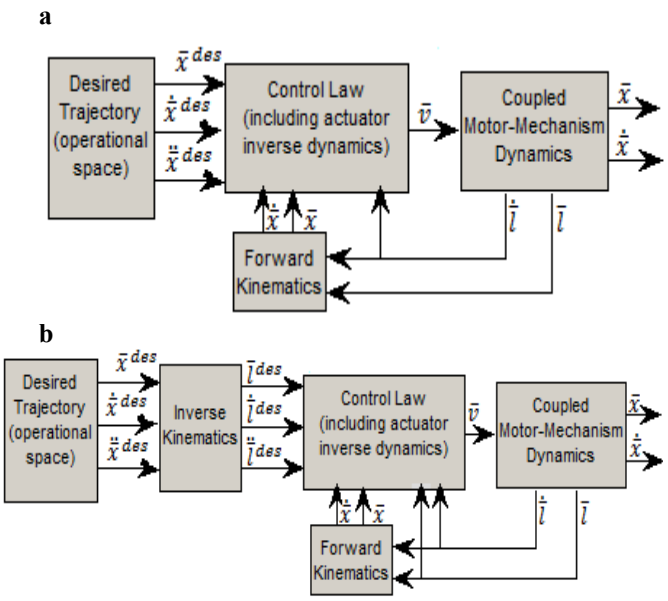

Figure 2-Alternative model-based control schemes: a) control in operational space, b) control in joint space

It is desired that the error asymptotically converges to zero according to:

$$\ddot{e} + K_v\dot{e} + K_p e = 0 \tag{9}$$

where K_p and K_v are 3×3 diagonal matrices which represent the control gains of the moving system. Since equation (9) is a second order differential equation, the control gains can be written in terms of closed-loop natural frequency and damping as follows:

$$\begin{aligned} K_p &= diag\{{\omega_1}^2, {\omega_2}^2, {\omega_3}^2\} \\ K_d &= diag\{2\zeta_1\omega_1, 2\zeta_2\omega_2, 2\zeta_3\omega_3\} \end{aligned} \tag{10}$$

The closed-loop natural frequency and damping are selected such that the desired response specifications are achieved.

The dynamics equation of the system as in (1) consists of a linear term $M(\bar{x})\ddot{\bar{x}}$ plus nonlinear terms $V(\bar{x}, \dot{\bar{x}}) + G(\bar{x}) + F_{fr}(\dot{\bar{x}})$. If τ is chosen such that it compensates for the nonlinear terms, the overall dynamic equation is a linear equation to which linear systems' control strategies can now be applied. By choosing τ in such a manner as:

$$\tau = V(\bar{x}, \dot{\bar{x}}) + G(\bar{x}) + F_{fr}(\dot{\bar{x}}) + \epsilon \tag{11}$$

the dynamic equation (1) is transformed to:

$$M(\bar{x})\ddot{\bar{x}} = \epsilon \tag{12}$$

where ϵ is the new control input. By choosing:

$$\epsilon = M(\bar{x})\left(\ddot{\bar{x}}^{des} + K_d\dot{e} + K_p e\right) \tag{13}$$

and substituting in (12) it is seen that (9) is obtained.

Therefore the control law box (see Figure 2) must produce a voltage to yield τ as computed in (11).

4. SIMULATION RESULTS

As already mentioned the command input to the platform is produced by motion cueing algorithms in operational variables i.e. z, φ, θ.

For the model-based control, as well as $\bar{x}^{des}$, $\dot{\bar{x}}^{des}$ and $\ddot{\bar{x}}^{des}$ must also be available and they must be obtained from the available data if they're not produced through the motion cueing algorithm. This can be done by numerical differentiation that involves large errors especially at the first intervals that cause malfunction of the controller in some cases. A better substitute for numerical differentiation is the derivative filter which is a first-order high-pass filter whose break frequency is chosen far enough from the system frequency [8].

For simulation a special platform is considered. The mass of the payload being equal to the mass of the cockpit and the pilot are assumed to be constant as there is little uncertainty in that due to the high known mass of the cockpit. The response of the system for several desired trajectories such as steps, ramps and sinusoidal inputs were examined. A desired trajectory for which the responses are presented is assumed as follows:

$$\begin{aligned} z_c(t) = z_{c1} + z_{c0}\sin(\omega_1 t + \phi_1), \quad \phi_c(t) = \varphi_{c0}\sin(\omega_2 t + \\ \phi_2), \quad \theta_c(t) = \theta_{c0}\sin(\omega_2 t + \phi_3) \end{aligned} \tag{14}$$

where z_{c1} is the z coordinate at neutral point, z_{c0}, φ_{c0} and θ_{c0} are trajectory amplitudes, ω_1 and ω_2 are the position and orientation trajectory frequencies and t is the time. The trajectory parameters for which the simulation results are presented, are as follows: $z_{c0} = 0.2\,m$, $\varphi_{c0} = 20^0$, $\theta_{c0} = 15^0$, $\omega_1 = 1\,rad/s$, $\omega_2 = 2\,rad/s$, $\phi_1 = \frac{\pi}{2}\,rad$, $\phi_2 = \frac{\pi}{6}\,rad$ and $\phi_3 = \frac{\pi}{3}\,rad$.

The controller is designed to yield a desired response specification of critical damping and 0.1 sec settling time which is adequate for our design purpose [15]. The controller gains determined to achieve the above control specifications are $K_p = 3364\,rad^2/s^2$ and $K_d = 116\,rad/s$.

The controller is then applied to the complete dynamics model that takes into account both the legs' mass and inertia and actuator frictions. The accuracy of the model was verified by comparison with an equivalent model built in simMechanics. For the platform used for simulations, legs' mass form %13 of the total payload mass. The output trajectories and the controlled system response errors are plotted in Figures 3 to 4 and closed-loop bode plots are presented in Figure 5.

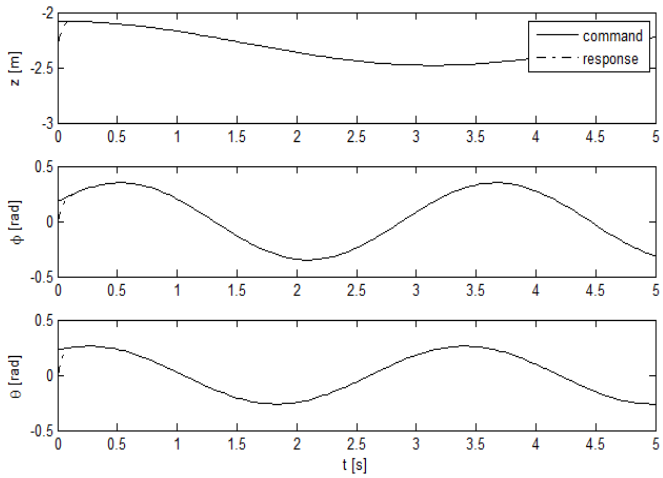

Figure 3-Platform response vs. desired trajectory for the system under model-based controller

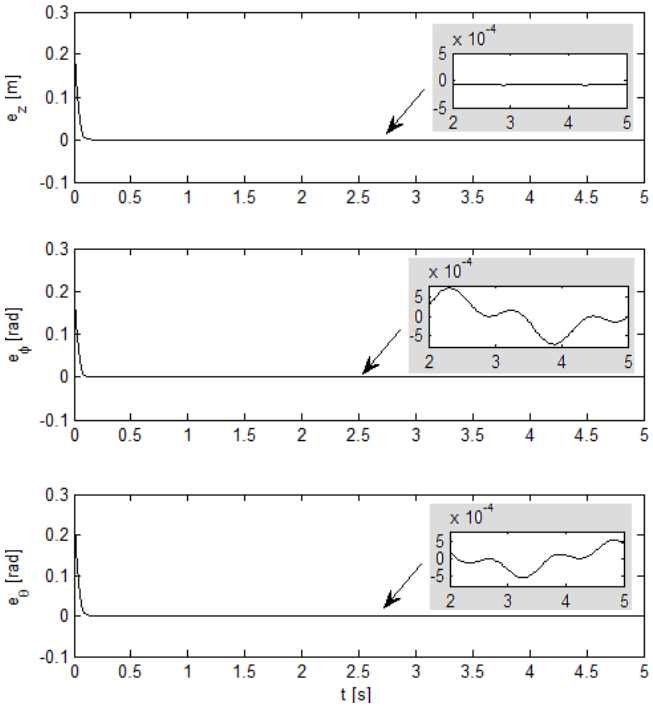

Figure 1-Error of platform position and orientation (z, φ and θ) for the system under model-based controller

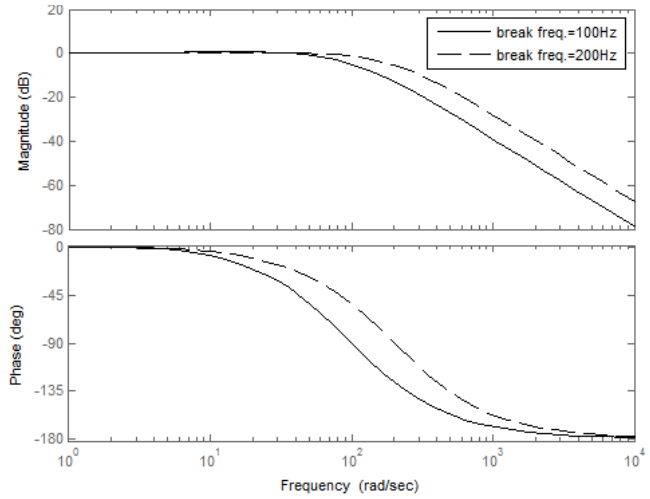

Figure 5-Bode plots of closed-loop transfer functions ($\frac{z}{z^c}, \frac{\phi}{\varphi^c}$ or $\frac{\theta}{\theta^c}$) for the system under model-based controls (model-based controller's derivative break frequency = 100 and 200 Hz.)

From Figure 4, it is seen that the error asymptotically decreases and reaches nearly zero as expected and the controlled system response coincides with the desired trajectory after the settling time of 0.1 second. The residual error is certainly due to the inexact correspondence of the simplified inverse dynamics used in the controller and the dynamics of the system to be controlled. Although legs form %13 percent of the total payload that does not seem to be negligible at the first glance, neglecting their dynamics in the controller is seen to lead to quite negligible error.

In addition, from the bode plots of the closed-loop system, it is clearly seen that a bandwidth of over 100 rad/s for this system can be achieved by a derivative filter's frequency of 100 Hz. This bandwidth can be further extended by increasing the filter's break frequency but at the expense of more computational effort and enhancing the stiffness of the system due to the existence of very fast state variables as well as the system's original states.

In the derivation of the inverse dynamics, legs' inertia were neglected. This extremely decreases the computational load of the model-based controller, making it an appropriate sufficiently- fast controller for real-time applications, while it only leads to quite negligible response error (see Figure 4). Since in many flight simulation applications the platform mass is much larger than the mass of the actuators [9], the preceding assumption is usually valid to be made to decrease computational burden without imposing considerable errors.

5. CONCLUSION

A heave-pitch-roll motion platform extensively used in flight simulators was considered. The mechanism introduces a novel configuration of the system that benefits in two aspects. First by applying a nearly constant upward force using a high capacity pneumatic actuator, the weight of the

platform and its payload is compensated for. It causes smaller loads to be transmitted to the electrically actuated jacks. Second by use of a new configuration of scissors, motion is constraint in heave direction with less friction and backlash and more stiffness, in comparison with the available similar mechanisms. Both these aspects result in a better control task, robustness in path following and capability of handling greater loads.

A nonlinear model-based controller was applied to the system. To derive the controller, a simplified dynamic model was obtained that considers the salient dynamics. It takes into account the actuation dynamics, the nonuniform distribution of payload and actuator friction but neglects the effect of legs' inertia.

The designed controller, when applied to the system, yields an overall linear closed-loop system that follows the command with an asymptotically convergent error that reaches zero after the chosen settling time. Due to overall linearity, the closed-loop system keeps its control specifications in entire the workspace. The controller also benefits by a relatively high bandwidth that can be further increased to a desired value by increasing the selected break frequency of derivative filter. It proves that for case of high-payload motion platforms where legs' mass and inertia and small uncertainties associated with payload and its center of mass do not have considerable effects on the inverse dynamics of the system, model-based controllers can efficiently be used in real-time controllers providing high precision motion following.

Appendix A.

For the platform sketched in Figure A.1, the equations of motion obtained from Euler law are as follows:

$$\left([m\tilde{D} \quad RI_{\bar{c}}{}^{m}]\begin{bmatrix}J_{c,x}\\ J_{\omega,x}\end{bmatrix}\right)\ddot{\bar{x}} = -([m\tilde{D} \quad RI_{\bar{c}}{}^{m}])\begin{bmatrix}b_{c,x}\\ b_{\omega,x}\end{bmatrix} + \tilde{D}\begin{bmatrix}0\\0\\mg\end{bmatrix} + \begin{bmatrix}0\\0\\M_z\end{bmatrix} - R(\bar{\omega}^m \times I_{\bar{c}}{}^{m}\bar{\omega}^m) + \begin{bmatrix}\tilde{D}_{f_1}\bar{l}_{n,1} & \tilde{D}_{f_2}\bar{l}_{n,2} & \tilde{D}_{f_3}\bar{l}_{n,3}\end{bmatrix}F_{fr}^{*} + \begin{bmatrix}\tilde{D}_{f_1}\bar{l}_{n,1} & \tilde{D}_{f_2}\bar{l}_{n,2} & \tilde{D}_{f_3}\bar{l}_{n,3}\end{bmatrix}F_a \qquad \text{(A.1)}$$

The equation of motion of the platform in z direction obtained from Newton law is as follows:

$$\left(m + M_{sync}(z_p)\right)\ddot{z} + M_{sync}[0\ 0\ 1]R\tilde{D}^m J_{\omega,x}\ddot{\bar{x}} = (m + m_{sync})g - C_{synch}(z_p, \dot{z}_p) + \sum(F_a)_z + F_{z_{p0}} + M_{sync}(z_p)[0\ 0\ 1]\left(R\tilde{\Omega}^{m^2}\bar{d}^m - R\tilde{D}^m b_{\omega,x}\right), \qquad (A.2a)$$

where $(F_a)_z$ are actuator forces' z components and

$$F_{z_{p0}} = F_{z_{const}} - b_{pnum}\dot{z}_p - f_{k_0}\frac{\dot{z}_p}{|\dot{z}_p|}. \qquad (A.2b)$$

where $F_{z_{const}}$ is the pneumatic actuator constant upward force, b is viscous friction constant and f_{k_0} , dry kinetic friction constant.

The following relations exist:

$$J_{\omega,x} = \begin{bmatrix}0 & 1 & 0\\ 0 & 0 & 1\\ 0 & 0 & -\tan\phi\end{bmatrix} \qquad \text{(A. 3a)}$$

$$J_{c,x} = \begin{bmatrix}-\begin{bmatrix}1 & 0 & 0\\ 0 & 1 & 0\end{bmatrix}R\tilde{D}^m J_{\omega,x}\\ [1 \quad 0 \quad 0]\end{bmatrix} \qquad (A.3b)$$

$$b_{\omega,x} = [0 \quad 0 \quad -(1+\tan^2\phi)pq\ ]^T \qquad (A.3c)$$

$$b_{c,x} = \begin{bmatrix}\begin{bmatrix}1 & 0 & 0\\ 0 & 1 & 0\end{bmatrix}\left\{R\tilde{\Omega}^{m^2}\bar{d}^m - R\tilde{D}^m b_{\omega,x}\right\}\\ 0\end{bmatrix} \qquad (A.3d)$$

The matrices defined in (1) are then obtained as:

$$M(\bar{x}) = \begin{bmatrix}(m + M_{sync})[1 \quad 0 \quad 0] + M_{sync}[0\ 0\ 1]R\tilde{D}^m J_{\omega,x}\\ \begin{bmatrix}1 & 0 & 0\\ 0 & 1 & 0\end{bmatrix}\left([m\tilde{D} \quad RI_{\bar{c}}{}^{m}]\begin{bmatrix}J_{c,x}\\ J_{\omega,x}\end{bmatrix}\right)\end{bmatrix} \qquad (A.4a)$$

$$V(\bar{x}, \dot{\bar{x}}) = \begin{bmatrix}M_{sync}[0\ 0\ 1]\left(R\tilde{\Omega}^{m^2}\bar{d}^m - R\tilde{D}^m b_{\omega,x}\right) - C_{synch}\\ -\begin{bmatrix}1 & 0 & 0\\ 0 & 1 & 0\end{bmatrix}\left\{([m\tilde{D} \quad RI_{\bar{c}}{}^{m}])\begin{bmatrix}b_{c,x}\\ b_{\omega,x}\end{bmatrix} + R(\bar{\omega}^m \times I_{\bar{c}}{}^{m}\bar{\omega}^m)\right\}\end{bmatrix} \qquad \text{(A. 4b)}$$

$$G(\bar{x}) = \begin{bmatrix}(m + m_{sync})g\\ \begin{bmatrix}1 & 0 & 0\\ 0 & 1 & 0\end{bmatrix}\tilde{D}\begin{bmatrix}0\\0\\mg\end{bmatrix}\end{bmatrix} \qquad (A.4c)$$

where the following notations have been used:

m Mass of total payload (platform and its payload)
M_{sync} Equivalent mass for inertia of scissors and gear set
m_{sync} Equivalent mass for gravity of scissors and gear set
C_{synch} Coriolis force of scissors mechanism
$I_{\bar{c}}^{m}$ Total payload matrix of moment inertia
$\bar{d}$ Displacement vector of total payload center of mass from pneumatic actuator upper joint
$\bar{a}_i{}^{m}$ Position vector of the upper joint of *i*th leg relative to the platform-fixed frame's origin
$\bar{l}_{n,i}$ The unit vector of *i*th leg directed from the lower joint to the upper joint
z z coordinate of the total payload center of mass in inertial frame
$\bar{\omega}$ Platform angular velocity in inertial frame
ϕ, θ Euler angles representing roll and pitch of the platform

$F_{z_{p0}}$ Pneumatic actuator force exerted to the platform through the upper joint

z_p z coordinate of the pneumatic actuator upper joint (point p)

$\dot{z}_p$ Pneumatic actuator upper joint velocity in z direction

$\bar{d}_{f_i}$ Displacement vector of the *i*th actuator upper joint from the pneumatic actuator upper joint

$\bar{a}^m$ Represents an arbitrary vector quantity $\bar{a}$ expressed in platform-fixed frame

$\tilde{A}$ The skew symmetric matrix designating the cross product of an arbitrary vector $\bar{a}$

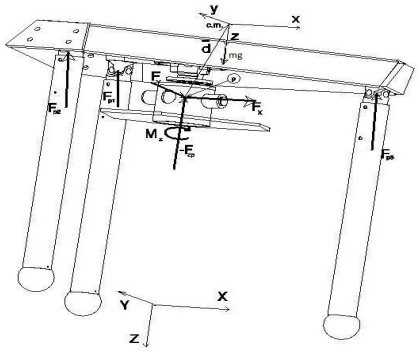

Figure A.1-Inertial and platform-fixed coordinate frames

Appendix B.

The mechanism characteristics are presented in this appendix.

Platform characteristics:

$m = 4000\ kg$

$M_{sync} = 185\ kg$

$m_{sync} = 116\ kg$

$$I_{\bar{c}}^{m} = \begin{bmatrix} 2.947 & 0 & 0 \\ 0 & 5.667 & 0 \\ 0 & 0 & 7.947 \end{bmatrix} \times 10^3\ kg.m^2$$

$\bar{d} = [0 \quad 0 \quad -0.61]^T\ m$

$\bar{a}_1^m = [-0.66 \quad -0.74 \quad 0.61]^T\ m$

$\bar{a}_2^m = [-0.66 \quad 0.74 \quad 0.61]^T\ m$

$\bar{a}_3^m = [\ 1.32 \quad 0 \quad 0.61]^T\ m$

$F_{z_{const}} = 4\ kN$, $b_{pnum.} = 920\ \frac{N.s}{m}$

PM DC motor characteristics:

$K_a = 0.668\ Nm/A$

$R_a = 0.51\ \Omega$

$L_a = 300 \times 10^{-6}\ H$

$K_b = 0.6685\ Vs/rad$

$J_m = 8.5 \times 10^{-3}\ kgm^2$

$b = 0.00105\ Nms/rad$

$r = 2\pi/0.005\ rad/m$

REFERENCES

[1] D. Stewart, A Platform with Six Degrees of freedom, Proc. Inst. Mech. Eng., Vol. 180, Part 1, No. 5, pp. 371-386, 1965.

[2] B. Dasgupta and T.S. Mruthyunjaya, The Stewart platform manipulator: A review, Mechanism and Machine Theory 35(1), 15-40, 2000.

[3] N. A. Pouliot, M. A. Nahon, and C. M. Gosselin; Analysis and comparison of the motion simulation capabilities of three-degree-of-freedom flight simulators, AIAA Flight Simulation Technologies Conference, Technical Papers (A96-35001 09-01), 1996.

[4] R. J. Telban, A nonlinear motion cueing algorithm with a human perception model, Phd. Thesis, Department of mechanical engineering, State university of New York, 2002.

[5] R. J. Telban and F. M. Cardullo, Motion Cueing Algorithm Development: Human-Centered Linear and Nonlinear Approaches, NASA/CR-2005-213747.

[6] Parallel Manipulators, Towards New Applications, ISBN 978-3-902613-40-0, pp: 269-294, 2008.

[7] Z. Qu, D. M. Dawson, Robust tracking control of robot manipulators, IEEE Press, 1996.

[8] Z. Yang, J. Wu; J. Mei, J. Gao and T. Huang, Mechatronic Model Based Computed Torque Control of a Parallel Manipulator, International journal of advanced robotic systems, vol. 5, No.1, pp:123-128, 2008.

[9] R. Kelly, V. Santibanez and A. Loria, Control of robot manipulators in joint space, Springer, 2005.

[10] I. Davliakos and E. Papadopoulos, Model-based control of a 6-dof electrohydraulic Stewart–Gough platform, Mechanism and Machine Theory, 2008.

[11] M. Idan and D. Sahar, A Robust Controller for a Dynamic Six Degrees of Freedom Flight Simulator, AIAA Flight Simulation Technologies Conference, San Diego, CA, pp. 53-60, 1996.

[12] L. Sciavicco and B. Siciliano, Modeling and control of robot manipulators, The McGraw-Hill Companies, Inc., 1996.

[13] M. Aminzadeh, A. Mahmoodi, M. Sabzehparavar. Dynamic analysis of a 3DoF Motion Platform. International Journal of Robotics, IJR08, 2009.

[14] I. Davliakos and E. Papadopoulos, Model-based position tracking control for a 6dof electrohydraulic Stewart platform, proceedings of the 15th Mediterranean conference on control and automation, 2007.

[15] S. H. Koekkebakker, Model-based control of a flight simulator motion system, Phd. Thesis, University of Delf, 2001.

BIOGRAPHY

Masoomeh Aminzadeh *is a MSC student at the Department of Aerospace Engineering, Amirkabir University of Technology where she also received her bachelor's degree in 2007. As an undergraduate student, she contributed to an industrial project on design of a fixed-base flight simulator of a turboprop aircraft. As a MSC student, she contributed to the design of a motion-based flight simulator as well as some other aerospace projects. Her research interests include robotic mechanisms, motion systems, modern and intelligent control, and system identification.*

Mehdi Sabzehparvar *is an associate professor at the Department of Aerospace Engineering, Amirkabir University of Technology. He received his PhD in Aerospace Engineering from Mississippi State University. He has tens of technical papers in aeronautical and aerospace field and has had leading contribution to many flight simulation industrial projects. His specialized research areas are flight simulation, navigation and aircraft system identification.*